Acta Geochim
https://doi.org/10.1007/s11631-020-00445-z

ORIGINAL ARTICLE

Helium and argon isotope geochemistry of the Tibetan Qulong porphyry Cu-Mo deposit, China

Keqiang Peng[1,2] · Liyan Wu[1] · Yong Huang[1] · Ke Jiang[3]

Received: 29 September 2020 / Revised: 7 November 2020 / Accepted: 17 November 2020

Abstract The Qulong porphyry Cu–Mo deposit, generated in the Miocene post-collisional extension environment of the Gangdese Copper (Molybdenum) Metallogenic Belt, is one of the largest porphyry Cu deposits in China. This study reports the noble gas isotopic compositions of volatiles released from fluid inclusion reserved in pyrite from the Qulong deposit. $^{3}He/^{4}He$ and $^{40}Ar/^{36}Ar$ ratios range from 0.54 to 1.015 Ra and 300–359, respectively. Concentrations of ^{4}He and ^{40}Ar range from 1.77 to 2.62×10^{-8} cm^3 STP and $1.7–34 \times 10^{-8}$ cm^3 STP, respectively. The isotopic composition of noble gases indicates that the ore-forming fluids of the Qulong Cu–Mo deposit were a mixture of fluid containing mantle component, which is exsolved from the porphyry magma, and crustal fluid characterized by atmospheric Ar and crustal radiogenic He. The $\delta^{34}S$ values of pyrite and molybdenite range from − 0.52‰ to 0.31‰, with an average of − 0.12‰, indicating a magmatic origin. More mantle components were involved in the Cu–Mo deposit than in the Mo–Cu deposit in the Qulong-Jiama ore-district.

Keywords He and Ar isotopes · Sulfur isotope · Qulong Cu–Mo deposit · Ore-forming fluid · Tibet · China

✉ Liyan Wu
wuliyan@mail.gyig.ac.cn

[1] State Key Laboratory of Ore Deposit Geochemistry, Institute of Geochemistry, Chinese Academy of Sciences, Guiyang 550081, China

[2] University of Chinese Academy of Sciences, Beijing 100049, China

[3] College of Eco-Environmental Engineering, Guizhou Minzu University, Guiyang 550025, China

1 Introduction

The Qulong porphyry Cu–Mo deposit (PCD), located in the east part of the Gangdese copper Metallogenic Belt, about 50 km east of Lhasa city, is one of the largest porphyry Cu deposits in China, with reserves of 10.6 Mt Cu@0.5% and 0.5 Mt Mo@0.03% (Xiao et al. 2012). Many studies have been done on the geology (Yang 2008; Yang et al. 2009; Qin et al. 2014), petrology (Hu et al. 2015; Mo et al. 2006; Yang et al. 2011), mineralization (Meng et al. 2006), geochronology (Meng et al. 2003; Wang et al. 2006; Li et al. 2017a, b), magmatic-hydrothermal evolution (Li et al. 2017a; Yang et al. 2005, 2009), and thermal history (Zhao et al. 2016; Zhou et al. 2019) of the Qulong deposit. Approximately the same S and Pb isotope compositions of sulfide and ore-related porphyry show that the ore-forming materials are mainly from the porphyry magma (Qu et al. 2002, 2007; Meng et al. 2006). However, the contribution of the mantle is not clear.

Among the noble gases, He and Ar are the most efficient for tracing the sources of ore-forming fluids because of the significant difference of isotopic compositions between end members. $^{3}He/^{4}He$ ratio of the upper mantle is 7–9 Ra (Graham, 2002, where Ra is the atmospheric $^{3}He/^{4}He$ ratio and $1\ Ra = 1.39 \times 10^{-6}$), while the $^{3}He/^{4}He$ ratio of crustal rocks is 0.01–0.05 Ra (O'Nions and Oxburgh 1983), $^{40}Ar/^{36}Ar$ ratio of air is 295.5, while mantle-derived Ar is dominated by radiogenic ^{40}Ar, with $^{40}Ar/^{36}Ar > 40{,}000$, and crustal rocks have $^{40}Ar/^{36}Ar \geq 45{,}000$ due to radiogenic and nucleogenic Ar produced in the crust. Therefore, $^{40}Ar/^{36}Ar$ ratios are sensitive to trace the addition of meteoric fluid from crust or mantle Ar, and the $^{3}He/^{4}He$ ratios can distinguish the involvement of mantle He (Stuart et al. 1995; Hu et al. 1998, 1999, 2004, 2009, 2012). Thus, He and Ar isotopes can provide a unique insight into the

Published online: 29 November 2020

origin and evolution of ore-forming fluids (Burnard et al. 1999; Burnard and Polya 2004; Davidheiser-Kroll et al. 2014; Hu et al. 2012; Kendrick et al. 2001; Stuart et al. 1995; Wu et al. 2018).

In this study, He and Ar isotopes of fluid inclusions in pyrites and S isotopic compositions of pyrite and molybdenite were obtained to constrain the origin of the ore-forming fluids of the Qulong PCD.

2 Geological background

The Qulong PCD is situated in the southern part of the Lhasa Terrane, which is bordered by the Bangong–Nujiang suture (BNS) in the north and the Indus–Yarlung suture (IYS) in the south (Fig. 1), and is composed mainly of the Paleozoic to Mesozoic marine clastic sedimentary rocks and volcanic rocks, and the Paleozoic to Cenozoic magmatic rocks, with the Precambrian basement known as the Nyainqêntanglha Group (Yang et al. 2009; Zhang et al. 2014). The Lhasa terrane and is divided into the northern, central, and southern Lhasa subterranes, separated by the Shiquan River–NamTso Mélange and the Luobadui–Milashan faults (Zhang et al. 2014). According to the zircon ε_{Hf} values and relevant Hf model ages, the south and north Lhasa subterranes are dominated by juvenile crustal blocks while the central Lhasa subterrane is characterized with ancient and locally reworked crust (Hou et al. 2015).

The southern Lhasa subterrane mainly consists of Gangdese volcanic-magmatic arc, dominated by the extensively distributed Early Cenozoic Linzizong volcanic succession and the Cretaceous-Tertiary granitic intrusions (Pan et al. 2004, Pan 2006; Zhu et al. 2008, 2013). The India–Asia collision initiated along the Indus—Yarlung Zangbo suture at around 65–55 Ma (Rowley 1996; Mo et al. 2003; Wang et al. 2003; Ding et al. 2005; Dong et al. 2006; Pan 2006; Zhu et al. 2011, 2013), followed later by the subduction of India continental plate at around 35 Ma (Ali and Aitchison 2008; Wang et al. 2014). The subsequent break off of the denser India plate beneath the Asia plate at 25–15 Ma (Aitchison et al. 2007; Van Hinsbergen et al. 2012), which triggered the generation of the Oligo–Miocene magmatic rocks associated with porphyry Cu-Mo deposits along the of the Gangdese porphyry copper belt (Hou et al. 2009; Van Hinsbergen et al. 2012; Wang et al. 2014; Li et al. 2017a, b), of which the Qulong deposit is the largest (Zheng et al. 2004; Qin et al. 2014). The porphyry magmatism culminated at 16 ± 1 Ma, ranging from 26 to 13 Ma, and the molybdenite Re–Os ages of the mineralization are from 17 to 14 Ma (Hou et al. 2015 and the references therein).

The central Lhasa subterrane is composed of many Miocene porphyry (20–16 Ma) Mo–Cu deposits, such as the Bangpu porphyry Mo–Cu deposit. Most of those deposits are situated along the southern margin and spatially associated with the reworked ancient crustal block (Hou et al. 2015). Sr–Nd isotope data indicate that those

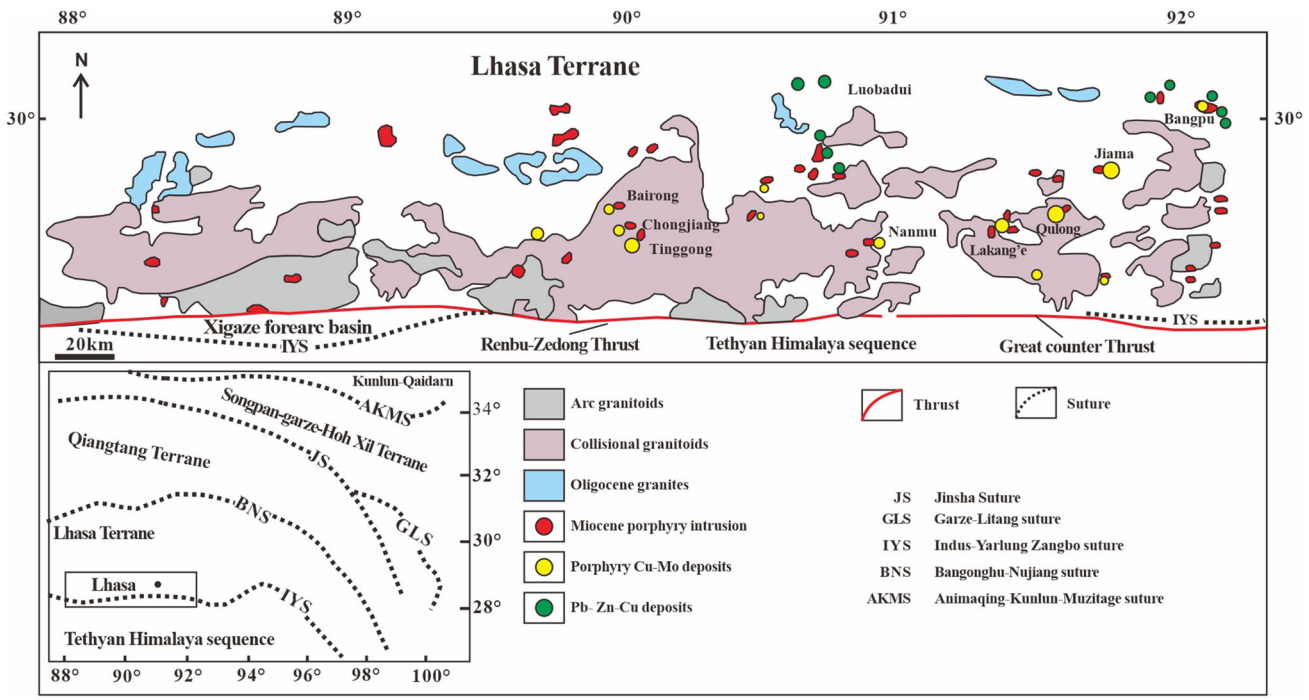

Fig. 1 Tectonic setting and geological map of the Gangdese Porphyry Copper Belt. Modified from Li et al. (2017b)

porphyry Mo deposits are possibly formed by the melting of an ancient lower crust with minor mantle component contribution (Hou et al. 2011, 2015).

3 Deposit geology

The outcrop layer of Jurassic Yeba Formation is widely distributed at the district of Qulong deposit, characterized by intermediate–acid volcanic rock, pyroclastic rock, and a few sedimentary rocks interbedded (Yang et al. 2009; Qin et al. 2014). The intrusive rocks at Qulong deposit are mainly the mid-Miocene intermediate–acid complex (Fig. 2), including the Rongmucuola pluton, the P porphyry, and the X porphyry. The mid-Miocene Rongmucuola pluton intruded into the Yeba Formation and the Jurassic dacite–rhyolite porphyry at 17.142 ± 0.014 Ma (Li et al. 2017b), which hosts the majority of the Cu–Mo in the Qulong deposit (Li et al. 2017a). It varies gradually from granodiorite to biotite monzogranite in composition (Yang et al. 2009; Zhao et al. 2016), containing plagioclase, K–feldspar, quartz, amphibole, and biotite in variable percentages (Zhao et al. 2016; Li et al. 2017b). The P porphyry (monzogranite porphyry), which was emplaced into the center of the western Rongmucuola pluton at 16.009 ± 0.016 Ma (Li et al. 2017b), is the syn-ore porphyry at the Qulong deposit (Yang et al. 2009; Hu et al. 2015; Zhao et al. 2016) and is composed of plagioclase (15 vol%), quartz (5 vol%), K–feldspar (5 vol%) and biotite (3 vol%) as phenocrysts, with the

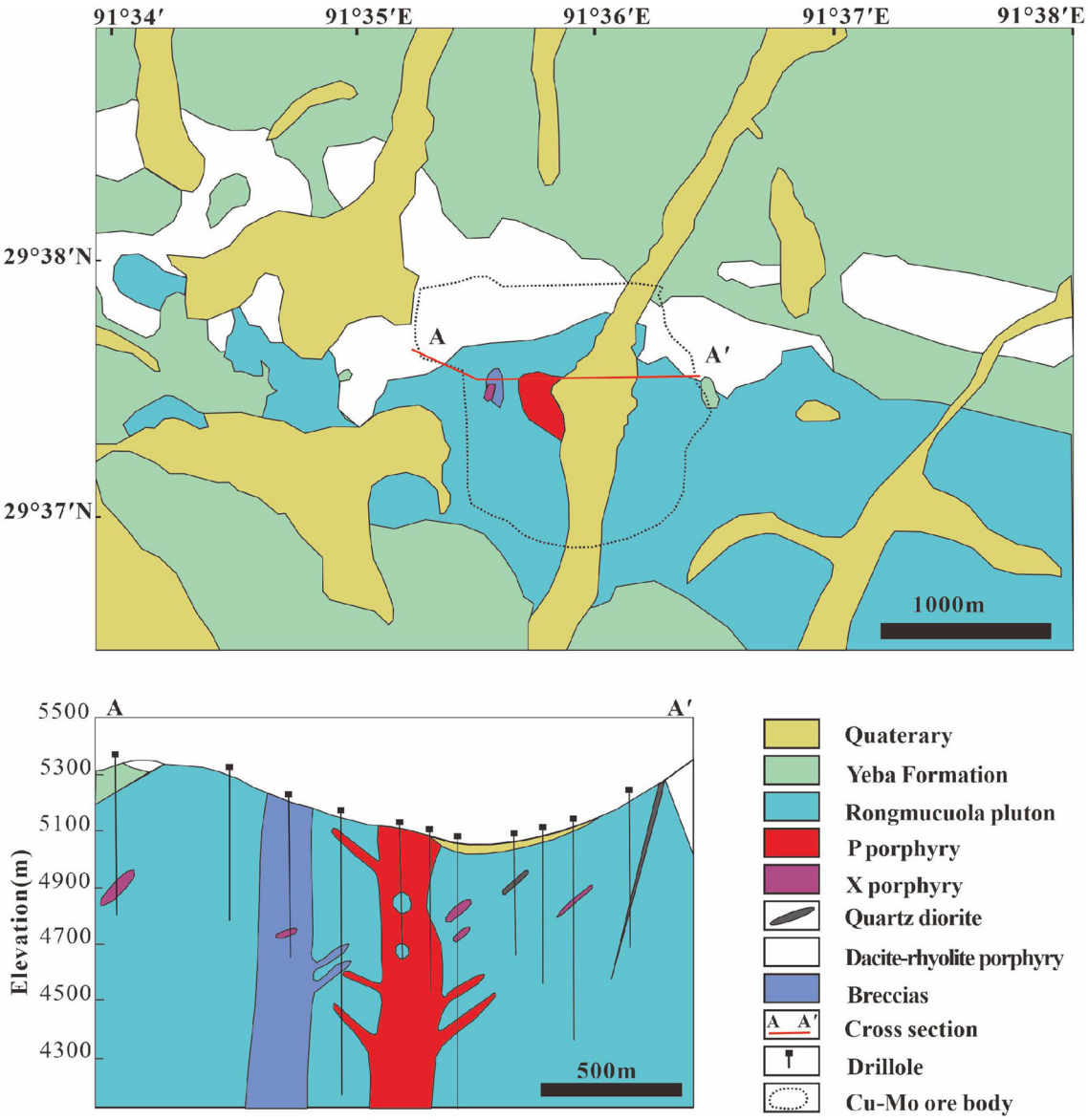

Fig. 2 Geological map **a** of the Qulong Cu–Mo porphyry deposit with cross-sections, **b**. Simplified and revised from Zhao et al. (2016)

quartz and feldspar, dominated the groundmass (Yang et al. 2009; Li et al. 2017a). The X porphyry (monzogranite porphyry), which crosscut both the western Rongmucuola pluton and the P porphyry, share a similar composition and texture with the P porphyry except that it contains less biotite.

The mineralization of Qulong PCD is mainly hosted in the western Rongmucuola pluton and associated with the potassic alteration minerals assemblages. The Re–Os age of molybdenite is 16.41 ± 0.48 Ma (Meng et al. 2003), and recently Li et al. (2017b) reported new high precision Re–Os age of 16.126 ± 0.008 Ma and 15.860 ± 0.010 Ma. The ore minerals at the Qulong deposit are dominated by pyrite, chalcopyrite and molybdenite (Fig. 3a, b, c) with minor bornite, galena and sphalerite (Fig. 3d), the mineralization occurs as veins (Fig. 3a, b) or disseminated. Most of the chalcopyrite and molybdenite are presented in veins that consist of quartz, pyrite and minor anhydrite (Fig. 3b). Chalcopyrite is either of disseminated structure that associated with biotite alteration, or occurs as veinlets with an alteration halo of chlorite–sericite. Molybdenite generally filled in the central or margin of quartz veins.

Fluid inclusion studies and H, O isotopic composition of Qulong deposit indicate that the ore–forming fluid of the early stage mineralization and alteration are exsolved from magma at the temperature of 550–650 °C with moderate salinity (9% NaCl), and mixed with meteoric water later (Li et al. 2018; Yang and Hou 2009). The S and Pb isotopes of copper–bearing porphyries and ore minerals from the deposit suggest that the ore–forming materials were mainly from magma (Meng et al. 2006).

4 Sampling and analytical methods

The samples used in this study were collected from drill cores of the Qulong Cu–Mo deposit (Fig. 3). Pure pyrite and molybdenite were hand-picked from the crushed ore under a binocular microscope. The measurements were carried out using a GV 5400 mass spectrometer at the Institute of Geochemistry, Chinese Academy of Sciences (IGCAS), Guiyang, China. The sensitivities of the GV5400 for He and Ar were 3.9725×10^{-4} A/Torr and 1.1018×10^{-3} A/Torr, respectively. Pure sulfide grains (1–2 g with sizes of 0.5–1.5 mm) were ultrasonically cleaned in alcohol before being loaded online into vacuum crusher buckets. The samples were baked at 120–150 °C in the crusher buckets for ca. 24 h to remove adhered atmospheric gases. The gases were released by sequential crushing of the pyrite grains in high–vacuum conditions. He and Ar isotopic compositions and abundances were calibrated against pipettes of 0.1 cm^3 STP air (5.2×10^{-7} cm^3 STP ^4He and 9.3×10^{-4} cm^3 STP ^{40}Ar). Procedural blanks were $< 2 \times 10^{-10}$ cm^3 STP ^4He and $(2–4) \times 10^{-10}$ cm^3 STP ^{40}Ar. The detailed analytical procedures are described in Hu et al. (2012).

The sulfur isotope composition of the sulfide minerals was determined using a Thermo MAT253 continuous flow isotope ratio mass spectrometer coupled to an elemental

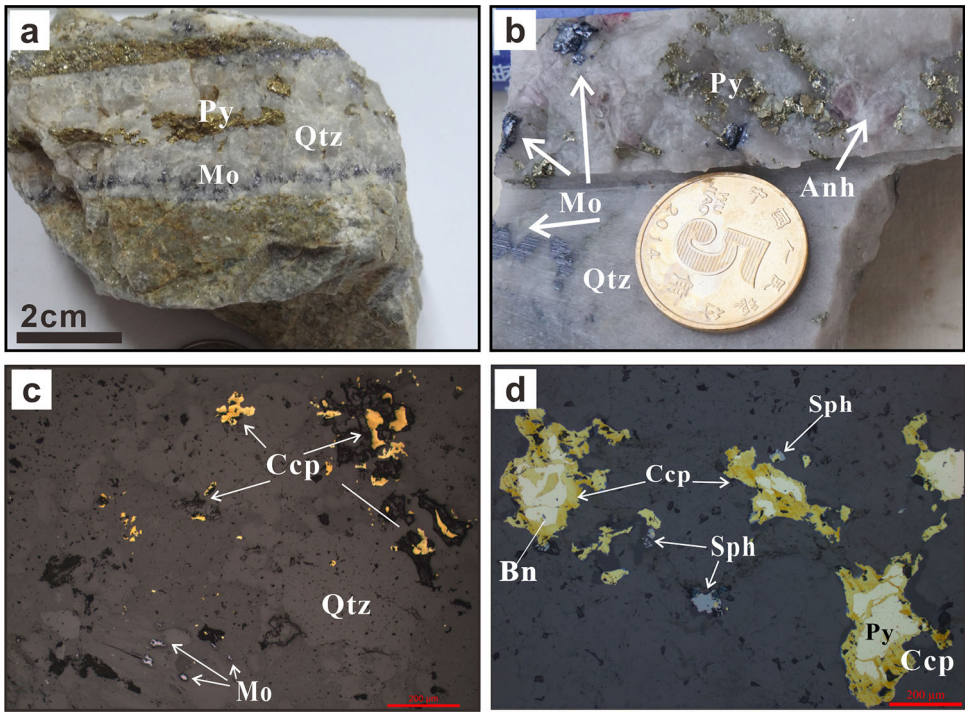

Fig. 3 Photographs of hand specimens and micrographs from the Qulong PCD. **a** Sample of Qtz-Py-Mo vein; **b** sample of Qtz-Py-Mo-Anh vein; **c** micrograph of Qtz- Mo-Ccp assemblage; **d** micrograph of Ccp-Bn-Sph-Py assemblage. Abbreviation: Anh-anhydrite, Bn-bonite, Ccp-chalcopyrite, Mo-molybdenite, Py-pyrite, Sph-sphalerite, Qtz-quartz

analyzer (EA–IRMS) at the IGCAS. Measurements are reported using standard δ–notation relative to V–CDT international standard. The reproducibility of replicate analyses of the IAEA international standards: IAEA S1 (− 0.3 ‰), IAEA S2 (+22.62 ‰), and IAEA S3 (− 32.49 ‰) yields a precision that is better than 0.2 ‰ (1σ).

5 Results

The He and Ar isotopic compositions released from the fluid inclusion of pyrite crystals are listed in Table 1 and Figs. 4, 5, and 6. The concentrations of ^{3}He vary from 4.68 to 14.17 × 10^{-15} cm^3 STP/g, and ^{40}Ar concentration range from 8.79 to 154.72 × 10^{-9} cm^3 STP/g. The $^{3}He/^{4}He$ ratios vary from 0.54 to 1.02 Ra (Ra: the $^{3}He/^{4}He$ ratio of air, 1 Ra = 1.39 × 10^{-6}), and the $^{40}Ar/^{36}Ar$ ratio varies from 300 to 359. $\delta^{34}S$ range from − 0.52 to 0.31 ‰, with an average of − 0.12 ‰.

6 Discussion

6.1 Source of ore-forming fluids using He, Ar, and S isotopes

Many studies have demonstrated that pyrite is capable of trap and preserve noble gases (Stuart et al. 1995; Hu et al. 1998, 2004, 2009, 2012; Burnard et al. 1999), and helium and argon trapped in fluid inclusion will not lose extensively within 100 Ma (Burnard et al. 1999). The ratios of $^{3}He/^{4}He$ and $^{40}Ar/^{36}Ar$ will not change even if the trapped He and Ar lost partially (Hu et al. 1997, 2004, 2012; Ballentine and Burnard 2002). Since pyrite is not Li-bearing mineral, there is no helium produced by the nuclear decay of lithium. Contamination of cosmogenic ^{3}He can also be eliminated since all of the pyrites of this study are collected from drill core of which the depths are more than 50 m. U and Th concentrations in hydrothermal fluids are commonly low (Hu et al. 2012; Norman and Musgrave 1994), therefore the radiogenic ^{4}He produced in situ in fluid inclusions is also negligible (Hu et al. 2012). The impact of ^{40}Ar produced by the decay of ^{40}K in the mineral lattice should be negligible because of the low diffusivity of Ar in pyrite (York et al. 1982; Smith et al. 2001) and the extremely low concentration of K in pyrite (York et al. 1982). The radiogenic ^{40}Ar produced in pyrite fluid inclusions is also negligible, due to the high proportion (more than 80%, see the Discussion in 5.1.2) of atmospheric Ar. Therefore, the measured He and Ar isotopic compositions of pyrite samples could basically represent the features of the ore–forming fluids of Qulong porphyry Cu–Mo deposit.

6.1.1 Helium

The $^{3}He/^{4}He$ ratios of pyrites from the Qulong PCD are between 0.54 and 1.01 Ra (Table 1; Fig. 5). By calculating the $F^{4}He$ values, which is defined as $^{4}He/^{36}Ar$ value of the sample relative to the atmospheric $^{4}He/^{36}Ar$ value of 0.1655 (Kendrick et al. 2001), we can determine the atmospheric Helium contribution. The $F^{4}He$ values of Qulong PCD are between 300 and 1920 (Table 1), indicating that ^{4}He of the Qulong PCD is 300–1900 times higher than the atmospheric concentration. This means that the atmospheric He contribution is negligible in the mineralizing fluids. The $^{3}He/^{4}He$ ratios of the Qulong PCD are significantly higher than the crustal fluid value (0.01–0.05Ra) and lower than the mantle components value (6–9 Ra), indicating that both mantle and crustal components were involved in the hydrothermal fluids of the Qulong PCD. The $^{3}He/^{4}He$ and $^{40}Ar/^{36}Ar$ ratios of Qulong PCD is plotted on the trend line (Fig. 5) modeled by binary mixing between a high $^{3}He/^{4}He$ (1.23 Ra), high $^{40}Ar/^{36}Ar$ fluid containing mantle component, and a crustal fluid with atmospheric $^{40}Ar/^{36}Ar$ and radiogenic ^{4}He (Burnard et al. 1999). The Qulong porphyry deposit is spatially and temporally associated with monzogranite porphyry (P porphyry) (Meng et al. 2003; Qin et al. 2014). S, Pb, H, and O isotopic features of the copper-bearing porphyries and ore minerals from the Qulong deposit show that ore-forming fluid and materials were mainly derived from the magma (Meng et al. 2006; Yang and Hou 2009). Therefore, the high $^{3}He/^{4}He$ ratio mantle end-member in the ore-forming fluid was likely to be exsolved from the monzogranite porphyry (P porphyry) magma. The $^{3}He/^{4}He$ ratio (1.02 Ra, the maximum value measured in this study) of the mantle end-member is much less than the typical sub-continental mantle value (∼ 6 Ra), indicating that the mantle helium from mantle-derived magma was diluted by incorporating radiogenic helium within the parental magma of the associated porphyry before helium was released into the hydrothermal system (Hu et al. 2012). This is consistent with the conclusion that monzogranite porphyry magma was generated by partial melting of the thickened lower–crust under the Tibetan orogen with the input of mantle components (Meng et al. 2006; Yang et al. 2015).

We can use the $^{3}He/^{4}He$ ratios to calculate the proportion of mantle and crustal components based on binary mixing. The proportion of mantle or crustal ^{4}He can be calculated using the following equation (Burnard et al. 1999):

$$^{4}He_{total} = {}^{4}He_{mantle} + {}^{4}He_{crust}$$
$$= {}^{4}He_{crust} + {}^{3}He_{mantle} \times \left(^{4}He/^{3}He\right)_{mantle}$$

Table 1 He, Ar and S isotopic compositions of sulfidesfrom the Qulong porphyry deposit

Sample	Mineral	Weight (g)	^{40}Ar (10^{-8} cm^3STP)	^{36}Ar (10^{-10} cm^3STP)	$^{40}Ar/^{36}Ar$	^{4}He (10^{-8} cm^3STP)	^{3}He (10^{-14} cm^3STP)	$^{3}He/^{4}He$ (Ra)	$^{36}Ar/^{3}He$	$F^{4}He$	$^{40}Ar^{*}/^{4}He$ (10^{-3})	$\delta^{34}S$ (‰)
zk816-1	Pyrite	4.16	18.6 ± 0.07	5.16 ± 0.07	359 ± 5	2.60 ± 0.08	1.95 ± 0.12	0.54 ± 0.04	26515	303	1271	− 0.52
ql1513	Pyrite	3.11	9.2 ± 0.04	2.82 ± 0.05	326 ± 5	2.62 ± 0.08	3.04 ± 0.14	0.83 ± 0.05	9283	561	325	0.24
zk1616-1	Pyrite	2.52	34.8 ± 0.14	10.4 ± 0.01	334 ± 3	2.18 ± 0.07	3.08 ± 0.14	1.02 ± 0.06	33,757	126	1843	− 0.05
zk816-2	Pyrite	1.94	1.7 ± 0.01	0.57 ± 0.29	300 ± 15	1.81 ± 0.05	2.52 ± 0.12	1.01 ± 0.06	2250	1922	15.1	− 0.19
ql1518	Pyrite	1.59	24.6 ± 0.10	8.18 ± 0.10	300 ± 3	1.77 ± 0.05	2.25 ± 0.12	0.91 ± 0.06	36,369	130	214	− 0.25
zk816-3	Pyrite											− 0.32
zk816-3	Molybdnite											− 0.48
QLD2	Pyrite											0.31
QLD2	Molybdnite											0.21

Errors quoted are at the 1σ confidence level

$^{40}Ar^{*}$is the non-atmospheric Ar, $^{40}Ar^{*} = {}^{40}Ar\text{-}[{}^{36}Ar \times 295.5]$

$F^{4}He=(^{4}He/^{36}Ar)_{sample}/(^{4}He/^{36}Ar)_{air}$, $(^{4}He/^{36}Ar)_{air}=0.1655$

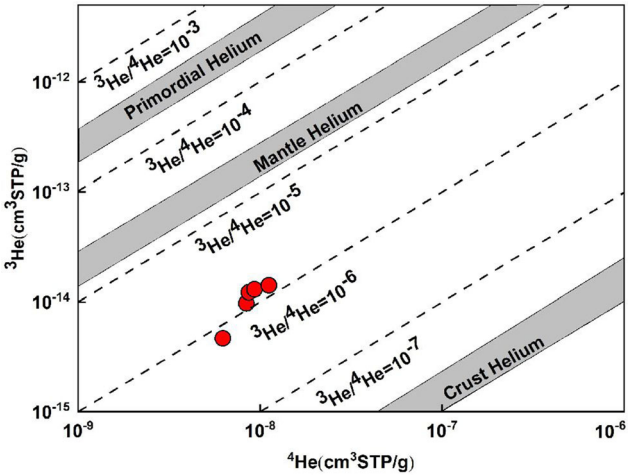

Fig. 4 Helium isotopes data of volatiles released from fluid inclusion of pyrite in the Qulong porphyry Cu–Mo deposit (modified from Mamyrin and Tolstikhin 1984)

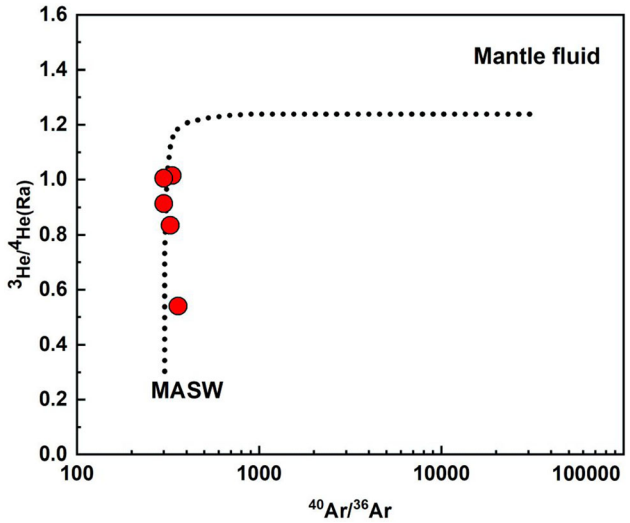

Fig. 5 $^{3}He/^{4}He$ versus $^{40}Ar/^{36}Ar$ for pyrite from the Qulong Cu–Mo deposit. He and Ar isotopic compositions of Qulong Cu–Mo deposit plotted on the trend line modelled by binary mixing between a "magmatic fluid" with $^{3}He/^{4}He$ = 1.23 Ra, $^{40}Ar/^{36}Ar \geq 40{,}000$ and a crust fluid with $^{40}Ar/^{36}Ar$ = 295.5, $^{3}He/^{4}He$ = 0.01 Ra. Modified from Burnard et al. (1999)

The total ^{4}He is measured from the samples; since ^{3}He are mainly from mantle so the measured ^{3}He could be regarded as mantle ^{3}He roughly. The mantle $^{4}He/^{3}He$ is about 1.19×10^{5} (Burnard et al.1999). According to the calculation, around 8%–90% ^{4}He was derived from the crust, corresponding to a mantle contribution of around 10%–16%.

6.1.2 Argon

The measured $^{40}Ar/^{36}Ar$ of Qulong deposit range from 300 to 359, which are higher than the value of air-saturated

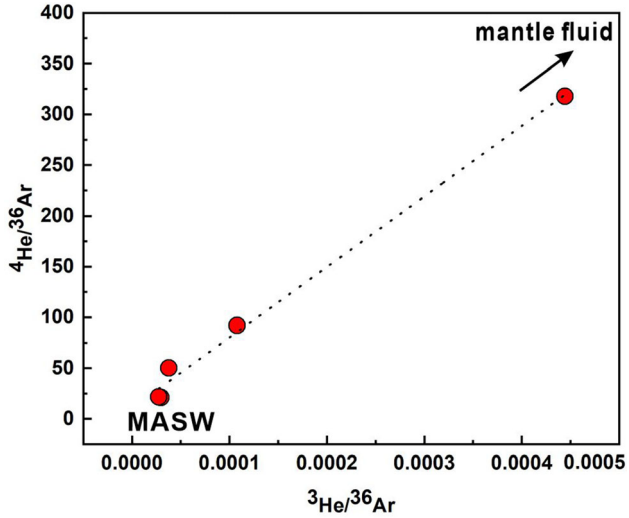

Fig. 6 $^{3}He/^{36}Ar$ versus $^{4}He/^{36}Ar$ for pyrite from the Qulong Cu–Mo deposit. The linear correlation is obtained by least squares regression: $^{4}He/^{36}Ar = 10.7 + 694{,}978 \times {}^{3}He/^{36}He$, $R^2 = 0.99$

water (ASW, $^{40}Ar/^{36}Ar$ = 295.5) and indicate the presence of excess $^{40}Ar^*$ derived from the mantle or crustal components. We can calculate the proportion of $^{40}Ar^*$ with the following equation (Kendrick et al. 2001):

$$^{40}Ar*\% = \frac{\left(^{40}Ar/^{36}Ar\right)\text{sample} - 295.5}{\left(^{40}Ar/^{36}Ar\right)\text{sample}} \times 100$$

Estimated $^{40}Ar^*$ range from 1.6% to 17%, with an average of 8.4%, which means that the proportion of air derived Ar is 83%–98.3%, with an average of 91.6%. Therefore, the ^{40}Ar of mineralization fluid of Qulong is dominated by atmospheric Ar that is commonly provided by the meteoric water. Since both ^{3}He and ^{36}Ar are unradiogenic, the $^{3}He/^{36}Ar$ ratio of meteoric water before mixing with mantle fluid is a constant value of 5×10^{-8} (Burnard et al. 1999). By extrapolating the trend in Fig. 6 to pure ASW ($^{3}He/^{36}Ar = 5 \times 10^{-8}$) generate a $^{4}He/^{36}Ar$ value of 10.7, which is much higher than that of ASW (0.46, Ozima and podosek 2002), indicating that the ASW was modified by the addition of radiogenic ^{4}He. Therefore, a crustal fluid end member consists of ASW modified by the crustal radiogenic ^{4}He, called modified air-saturated water (MASW), is considerable. Two samples have high $^{40}Ar^*/^{4}He$ ratios (Fig. 7) that much higher than that of the mantle and crust production ratios (0.5 and 0.2 respectively). The higher $^{40}Ar^*/^{4}He$ ratios may cause by the addition of a third source for $^{40}Ar^*$ or loss of He. The measured ^{4}He values are an order of magnitude lower than other deposit in this area (such as Bangpu deposit, Wang et al. 2015), therefore the higher $^{40}Ar^*/^{4}He$ ratios may because of boiling of the ore-forming fluid, which causes the enrichment of less volatile heavier noble gases in the

residue fluid and the lighter and more volatile noble gases enriched in the vapor phase (Kendrick et al. 2001). This is consistent with the fluid inclusion studies that boiling occurred in the early stage fluid (Yang and Hou 2009).

6.1.3 Sulfur

The $\delta^{34}S$ values of sulfides from the Qulong Cu–Mo deposit have a narrow range (− 0.52 ‰–0.31 ‰) and are within the range of the magmatic value (0 ‰ ± 2 ‰; Kyser 1990), indicating a magmatic origin. This may due to the low concentration in the MASW compared with the magmatic hydrothermal fluid. In addition, the country rocks of the deposit are mainly volcanic rocks so that the contamination of sulfur from these rocks would not change the S isotopic compositions of magma.

6.2 Comparison between porphyry Cu and Mo deposits in the Gangdese belt

Bangpu is a Mo-dominant with Cu as a by-product deposit in Qulong–Jiama ore–district in Gangdese metallogenic belt. The $^{3}He/^{4}He$ ratios of Bangpu (0.12–0.36 Ra) are lower than that of Qulong deposit (0.54–1.02 Ra), and the estimated proportion of crustal derived He for the Bangpu deposit and the Qulong deposit is 94%–98% and 84%–90%, respectively, which means Qulong deposit contains more mantle components compared with the Bangpu deposit, which is consistent with the results of Pb isotopes (Yao et al. 2002; She et al. 2005; Li et al. 2012; Zhou et al. 2012; Meng et al. 2006). This is coincident with the fact that the mineralization of the Qulong deposit is due to the refertilization of Cu in the juvenile lower crust with

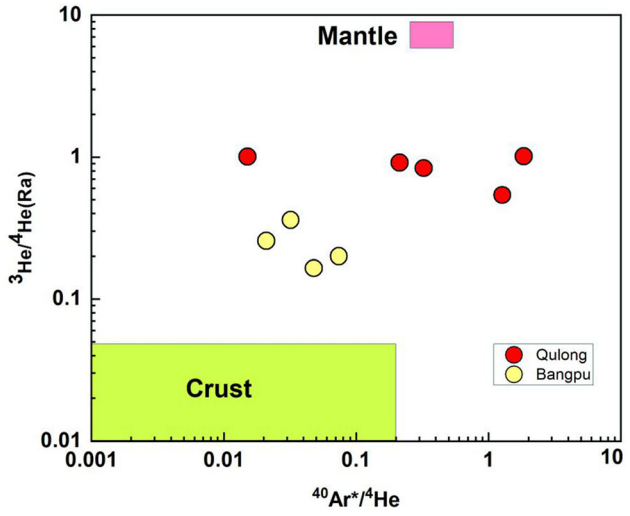

Fig. 7 $^{40}Ar^{*}/^{4}He$ versus $^{3}He/^{4}He$ for sulfides from the Qulong Cu–Mo and Bangpu Mo–Cu deposits in Gangdese metallogenic belt. Data of Bangpu porphyry Mo deposit collected from Wang et al.(2015)

significant mantle components, whereas the Bangpu porphyry Mo deposit is related to remelting of an ancient lower crust with minor mantle component contributions (Hou et al. 2013, 2015).

7 Conclusion

The ore-forming fluids of the Qulong Cu–Mo deposit were a mixture of a fluid containing mantle components and a crustal fluid containing atmospheric Ar and crustal radiogenic ^{4}He. The former was probably exsolved from the ore-bearing porphyry magma, and the later was meteoric water interacted with crustal rocks, therefore modified by the addition of radiogenic ^{4}He. $\delta^{34}S$ values of sulfides from Qulong deposit indicate that the sulfur is of magmatic origin and crustal fluid does not supply significant S to the ore-forming system. Mantle-derived components played an important role in the formation of Miocene deposits in the Gangdese metallogenic belt. Cu–Mo deposit contains much more mantle components compared with the Mo–Cu deposit.

Acknowledgements We wish to express our thanks to Dr. Guohao Jiang for He and Ar isotope analyses and Dr. Jing Gu for S isotope analysis. We thank Dr. Jingjing Zhu and an anonymous reviewer for their helpful comments which have improved the manuscript. This work was financially supported by the Strategic Priority Research Program (B) of Chinese Academy of Sciences (XDB18000000), National Natural Science Foundation of China (41773048) and The Western Young Scholars Project (Class A) of Chinese Academy of Sciences.

Compliance with ethical standards

Conflict of interest The authors declare that there is no conflict of interest.

References

Aitchison JC, Ali JR, Davis AM (2007) When and where did India and Asia collide? Geophys Res 112:1–19

Ali JR, Aitchison JC (2008) Gondwana to Asia: plate tectonics, paleogeography and the biological connectivity of the Indian sub-continent from the Middle Jurassic through Latest Eocene (166–35 Ma). Earth-Sci Rev 88(3–4):145–166

Ballentine CJ, Burnard PG (2002) Production, release and transport of noble gases in the continental crust. Rev Mineral Geochem 47(1):481–538

Burnard PG, Polya DA (2004) Importance of mantle derived fluids during granite associated hydrothermal circulation: He and Ar isotopes of ore minerals from Panasqueira. Geochim Cosmochim Acta 68(7):1607–1615

Burnard PG, Hu RZ, Turner G, Bi XW (1999) Mantle, crustal and atmospheric noble gases in Ailaoshan gold deposits, Yunnan Province, China. Geochim Cosmochim Acta 63(10):1595–1604

Davidheiser-Kroll B, Stuart FM, Boyce AJ (2014) Mantle heat drives hydrothermal fluids responsible for carbonate-hosted base metal

deposits: evidence from $^{3}He/^{4}He$ of ore fluids in the Irish Pb–Zn ore district. Miner Deposita 49(5):547–553

Ding L, Kapp P, Wan X (2005) Paleocene-Eocene record of ophiolite obduction and initial India-Asia collision, south central Tibet. Tectonics 24 (3):n/a-n/a

Dong FL, Hou ZQ, Gao YF, Zeng PS, Jiang CX (2006) Cenozoic granitoid in Tengchong, western Yunnan: genesis type and implication for tectonics. Acta Petrol Sin 22(4):927–937 (in Chinese with English abstract)

Graham DW (2002) Noble gas isotope geochemistry of mid-ocean ridge and ocean island basalts: characterization of mantle source reservoirs. Rev Miner Geochem 47(1):247–317

Hou ZQ, Yang Z, Qu X, Meng X, Li Z, Beaudoin G, Zaw K (2009) The Miocene Gangdese porphyry copper belt generated during post-collisional extension in the Tibetan Orogen. Ore Geol Rev 36(1–3):25–51

Hou ZQ, Zhang HR, Pan XF, Yang ZM (2011) Porphyry Cu (–Mo–Au) systems in non-arc settings, examples from the Tibetan Himalayan orogens and the Yangtze block. Ore Geol Rev 39:21–45

Hou ZQ, Zheng Y, Yang Z, Rui Z, Zhao Z, Jiang S, Sun Q (2013) Contribution of mantle components within juvenile lower-crust to collisional zone porphyry Cu systems in Tibet. Miner Deposita 48(2):173–192

Hou ZQ, Duan L, Lu Y, Zheng Y, Zhu D, Yang Z, McCuaig TC (2015) Lithospheric architecture of the Lhasa terrane and its control on ore deposits in the Himalayan-Tibetan orogen. Econ Geol 110(6):1541–1575

Hu RZ, Bi XW, Shao SX, Turner G, Burnard PG (1997) Helium isotopic compositions in the Machangqing copper deposit Yunnan Province. Chinese Sci Bull 42(17):1542–1545 **(in Chinese with English abstract)**

Hu RZ, Burnard PG, Turner G, Bi XW (1998) Helium and argon isotope systematics in fluid inclusions of Machangqing copper deposit in west Yunnan Province, China. Chem Geol 146(1–2):55–63

Hu RZ, Bi XW, Turner G, Burnard PG (1999) He and Ar isotope geochemistry of gold ore forming fluids in ailaoshan Gold Deposit. Sci China Earth Sci 29(4):321–330 **(in Chinese)**

Hu RZ, Burnard PG, Bi XW, Zhou MF, Pen JT, Su WC, Wu KX (2004) Helium and argon isotope geochemistry of alkaline intrusion-associated gold and copper deposits along the Red River-Jinshajiang fault belt, SW China. Chem Geol 203(3–4):305–317

Hu RZ, Burnard PG, Bi XW, Zhou MF, Peng JT, Su WC, Zhao JH (2009) Mantle-derived gaseous components in ore-forming fluids of the Xiangshan uranium deposit, Jiangxi province, China: evidence from He, Ar and C isotopes. Chem Geol 266(1–2):86–95

Hu RZ, Bi XW, Jiang GH, Chen HW, Peng JT, Qi YQ, Wei WF (2012) Mantle-derived noble gases in ore-forming fluids of the granite-related Yaogangxian tungsten deposit, Southeastern China. Miner Deposita 47(6):623–632

Hu YB, Liu JQ, Ling MX, Ding W, Liu Y, Zartman RE, Ma XF, Liu DY, Zhang CC, Sun SJ, Zhang LP, Wu K, Sun WD (2015) The formation of Qulong adakites and their relationship with porphyry copper deposit: geochemical constraints. Lithos 220:60–80

Kendrick MA, Burgess R, Pattrick RAD, Turner G (2001) Fluid inclusion noble gas and halogen evidence on the origin of Cu-Porphyry mineralising fluids. Geochim Cosmochim Acta 65(16):2651–2668

Kyser TK (1990) Stable isotopes in the continental lithospheric mantle. In: Menzies MA (ed) Continental mantle. Clarendon Press, Oxford, pp 127–156

Li YS, Lü ZC, Yan GS, Zhen SM, Du ZZ (2012) Isotopic characteristics of S, Pb, H and O of Jiama copper polymetallic ore deposit, Tibet and their significance. Earth Sci Front 19:72–81 **(in Chinese with English abstract)**

Li Y, Selby D, Condon D, Tapster S (2017a) Cyclic magmatic-hydrothermal evolution in porphyry systems: high-precision U–Pb and Re–Os geochronology constraints on the Tibetan Qulong porphyry Cu–Mo deposit. Econ Geol 112(6):1419–1440

Li Y, Selby D, Feely M, Costanzo A, Li XH (2017b) Fluid inclusion characteristics and molybdenite Re–Os geochronology of the Qulong porphyry copper-molybdenum deposit, Tibet. Miner Deposita 52(2):137–158

Li Y, Li XH, Selby D, Li JW (2018) Pulsed magmatic fluid release for the formation of porphyry deposits: tracing fluid evolution in absolute time from the Tibetan Qulong Cu–Mo deposit. Geology 46(1):7–10

Mamyrin BA, Tolstikhin IN (1984) Helium isotopes in natures. Elsevier, Amsterdam, pp 1–248

Meng XJ, Hou ZQ, Gao YF, Huang W, Qu XM, Qu WJ (2003) Re–Os dating for molybdenite from Qulong porphyry copper deposit in Gangdese metallogenic belt, Xizang and its metallogenic significance. Geol Rev 49:660–666 **(in Chinese with English abstract)**

Meng XJ, Hou ZQ, Li ZQ (2006) Sulfur and lead isotope compositions of the Qulong porphyry copper deposit, Tibet: implications for the sources of plutons and metals in the deposit. Acta Geol Sin 80(4):560–569 **(in Chinese with English abstract)**

Mo XX, Zhao ZD, Deng JF, Dong GC, Zhou S, Guo TY, Zhang SQ, Wang LL (2003) Response of volcanism to the India-Asia collision. Earth Sci Front 10:135–148 (in Chinese with English abstract)

Mo JH, Liang HY, Yu HX, Xie YW, Zhang YQ (2006) Composition of ELA-ICP-MS and SHRIMP U-Pb zircon ages of the Chongjiang and Qulong ore-bearing porphyries in the Gangdese porphyry copper belt. Geotectonic et Metallogenia 30(4):504–509 **(in Chinese with English abstract)**

Norman DI, Musgrave JA (1994) N_2–Ar–He compositions in fluid inclusions: indicators of fluid source. Geochim Cosmochim Acta 58(3):1119–1131

O'nions RK, Oxburgh ER (1983) Heat and helium in the Earth. Nature 306(5942):429–431

Ozima M, Podosek FA (2002) Noble gas geochemistry. Cambridge University Press, Cambridge, pp 1–286

Pan GT (2006) Spatial temporal framework of the Gangdese Orogenic Belt and its evolution. Acta Pet Sin 22:521–533

Pan GT, Ding J, Yao DS, Wang L (2004) Geological map of the Qinghai-Xizang (Tibet) plateau and adjacent areas. Chengdu Cartographic Publishing House, Chengdu, pp 1–133 **(in Chinese)**

Qin KZ, Xia DX, Li GM, Xiao B, Duo J, Jiang GW, Zhao JX (2014) Qulong Porphyry-Skarn Cu-Mo Deposit. Tibet. Science Press, Beijing, pp 1–316 **(in Chinese)**

Qu XM, Hou ZQ, Li YG (2002) Implication of S and Pb isotopic compositions of the Gangdise porphyry copper belt for the ore-forming material source and material recycling within the orogenic belt. Geol Bull China 21(11):765–766 **(in Chinese with English abstract)**

Qu XM, Hou ZQ, Khin Z, Li YG (2007) Characteristics and genesis of Gangdese porphyry copper deposits in the southern Tibetan Plateau: preliminary geochemical and geochronological results. Ore Geol Rev 31(1):205–223

Rowley DB (1996) Age of initiation of collision between India and Asia: A review of stratigraphic data. Earth Planet Sci Lett 145(1–4):1–13

She HQ, Feng CY, Zhang DQ, Pan GT, Li GM (2005) Characteristics and metallogenic potential of skarn copper–lead–zinc

polymetallic deposits in central eastern Gangdese. Miner Deposita 24:508–520 **(in Chinese with English abstract)**

Smith PE, Evensen NM, York D, Szatmari P, de Oliveira DC (2001) Single-crystal ^{40}Ar–^{39}Ar dating of pyrite: no fool's clock. Geology 29(5):403–406

Stuart FM, Burnard PG, Taylor REA, Turner G (1995) Resolving mantle and crustal contributions to ancient hydrothermal fluids: He–Ar isotopes in fluid inclusions from Dae Hwa W–Mo mineralisation, South Korea. Geochim Cosmochim Acta 59(22):4663–4673

Van Hinsbergen DJ, Lippert PC, Dupont-Nivet G, McQuarrie N, Doubrovine PV, Spakman W, Torsvik TH (2012) Greater India Basin hypothesis and a two-stage Cenozoic collision between India and Asia. Proc Natl Acad Sci 109(20):7659–7664

Wang CS, Li XH, Hu XM (2003) Age of intial collision of India with Asia: review and constraints from sediments in Southern Tibet. Acta Geol Sin 77(1):16–24 (**in Chinese with English abstract**)

Wang LL, Mo XX, Li B, Dong GC, Zhao ZD (2006) Geochronology and geochemistry of the ore-bearing porphyry in Qulong Cu (Mo) ore deposit, Tibet. Acta Pet Sin 22(4):1001–1008 **(in Chinese with English abstract)**

Wang R, Richards JP, Hou ZQ (2014) Extent of underthrusting of the Indian plate beneath Tibet controlled the distribution of Miocene porphyry Cu–Mo ± Au deposits. Miner Deposita 49(2):165–173

Wang L, Tang J, Cheng W, Chen W, Zhang Z, Lin X, Yang C (2015) Origin of the ore-forming fluids and metals of the Bangpu porphyry Mo–Cu deposit of Tibet, China: constraints from He–Ar, H–O, S and Pb isotopes. J Asian Earth Sci 103:276–287

Wu LY, Hu RZ, Li XF, Stuart FM, Jiang GH, Qi YQ, Zhu JJ (2018) Mantle volatiles and heat contributions in high sulfidation epithermal deposit from the Zijinshan Cu–Au–Mo–Ag orefield, Fujian Province, China: evidence from He and Ar isotopes. Chem Geol 480:58–65

Xiao B, Qin KZ, Li GM, Li JX, Zhao JX (2012) Highly oxidized magma and fluid evolution of Miocene Qulong giant porphyry Cu–Mo deposit, southern Tibet, China. Resour Geol 62(1):4–18

Yang ZM (2008) The Qulong giant porphyry copper deposit in Tibet: magmatism and mineralization. Unpublished Ph. D. Thesis, Chinese Academy of Geological Sciences, Beijing, China (**in Chinese with English abstract)**

Yang ZM, Hou ZQ (2009) Genesis of giant porphyry Cu deposit at Qulong, Tibet: constraints from fluid inclusions and H–O isotopes. Acta Geol Sin 83(12):1838–1859 **(in Chinese with English abstract)**

Yang ZM, Xie YL, Li GM, Xu JH (2005) Characteristics and forming process of ore-forming fluids at Qulong copper deposit in Gangdese porphyry copper belt, Tibet. Geol Prospect 41(2):21–26 **(in Chinese with English abstract)**

Yang ZM, Hou ZQ, White NC, Chang ZS, Li ZQ, Song YC (2009) Geology of the post-collisional porphyry copper–molybdenum deposit at Qulong, Tibet. Ore Geol Rev 36(1–3):133–159

Yang ZM, Hou ZQ, Jiang YF, Zhang HR, Song YC (2011) Sr-Nd-Pb and zircon Hf isotopic constrints on petrogenesis of the Late Jurassic granitic porphyry at Qulong, Tibet. Acta Pet Sin 27(7):2003–2010 **(in Chinese with English abstract)**

Yang ZM, Lu YJ, Hou ZQ, Chang ZS (2015) High-Mg diorite from Qulong in southern Tibet: implications for the genesis of adakite-like intrusions and associated porphyry Cu deposits in collisional orogens. J Pet 56(2):227–254

Yao P, Zheng MH, Peng YM, Li JG, Su DK, Fan WY (2002) Sources of ore-forming materials and the Genesis of the Jiama copper and polymetallic deposit in Gangdise island-arc belt, Xizang. Geol Rev 48:468–479 **(in Chinese with English abstract)**

York D, Masliwec A, Kuybida P, Hanes JA, Hall CM, Kenyon WJ, Scott SD (1982) $^{40}Ar/^{39}Ar$ dating of pyrite. Nature 300(5887):52–53

Zhang ZM, Dong X, Santosh M, Zhao GC (2014) Metamorphism and tectonic evolution of the Lhasa terrane, Central Tibet. Gondwana Res 25(1):170–189

Zhao JX, Qin KZ, Xiao B, McInnes B, Li GM, Evans N, Cao MJ, Li JX (2016) Thermal history of the giant Qulong Cu–Mo deposit, Gangdese metallogenic belt, Tibet: constraints on magmatic–hydrothermal evolution and exhumation. Gondwana Res 36:390–409

Zheng YY, Xue YX, Cheng LJ, Fan ZH, Gao SB (2004) Finding, characteristics and significances of Qulong superlarge porphyry copper (molybdenum) deposit, Tibet. Earth Sci Rev 29:103–108 **(in Chinese with English abstract)**

Zhou X, Wen CQ, Zhang XQ, Zhang Y, Fei GC, Wen Q (2012) Geochemical characteristics of sulfur and lead isotopes from the Bangpu Mo–Cu polymetallic deposit, Tibet. Geol Explor 48:24–30 **(in Chinese with English abstract)**

Zhou A, Dai JG, Li YL, Li HA, Tang JX, Wang CS (2019) Differential exhumation histories between Qulong and Xiongcun porphyry copper deposits in the Gangdese copper metallogenic Belt: insights from low temperature thermochronology. Ore Geol Rev 107:801–819

Zhu DC, Pan GT, Chung SL, Liao ZL, Wang LQ, Li GM (2008) SHRIMP zircon age and geochemical constraints on the origin of Lower Jurassic volcanic rocks from the Yeba Formation, southern Gangdese, South Tibet. Int Geol Rev 50(5):442–471

Zhu DC, Zhao ZD, Niu Y, Mo XX, Chung SL, Hou ZQ, Wang LQ, Wu FY (2011) The Lhasa Terrane: record of a microcontinent and its histories of drift and growth. Earth Planet Sc Lett 301(1–2):241–255

Zhu DC, Zhao ZD, Niu Y, Dilek Y, Hou ZQ, Mo XX (2013) The origin and pre-Cenozoic evolution of the Tibetan Plateau. Gondwana Res 23(4):1429–1454